

# Substrate independence of THz vibrational modes of polycrystalline thin films of molecular solids in waveguide THz-TDS

S. Sree Harsha,<sup>1</sup> Joseph. S. Melinger,<sup>2</sup> S. B. Qadri,<sup>3</sup> and D. Grischkowsky<sup>1,a)</sup>

<sup>1</sup>*School of Electrical and Computer Engineering, Oklahoma State University, Stillwater, Oklahoma 74078, USA*

<sup>2</sup>*Electronics Science and Technology Division, Code 6812, Naval Research Laboratory, Washington, D.C. 20375, USA*

<sup>3</sup>*Materials Science and Technology Division, Code 6366, Naval Research Laboratory, Washington, D.C. 20375, USA*

(Received 24 October 2011; accepted 14 December 2011; published online 23 January 2012)

The influence of the metal substrate on the measurement of high resolution THz vibrational modes of molecular solids with the waveguide THz-TDS technique is investigated. The sample film of salicylic acid is studied using waveguide THz-TDS on three different metal substrates and two-surface passivated substrates. The independence of the observed THz vibrational modes to the metal substrate is demonstrated. Independently, surface passivation is presented as a viable experimental addition to the waveguide THz-TDS technique to aid the characterization of samples with known reactivity to metal surfaces. © 2012 American Institute of Physics. [doi:10.1063/1.3678000]

## I. INTRODUCTION

Waveguide THz-TDS has been developed as a spectroscopic tool to obtain high resolution and significantly narrow resonance features of molecular solids in the THz spectral region. The demonstration of dispersion free and low loss propagation of broadband THz pulses as a TEM mode in the metal parallel plate waveguide (PPWG)<sup>1</sup> forms the basis for this technique, wherein the sub-wavelength confinement of the THz pulses between the metal plates of the PPWG is exploited to perform sensitive spectroscopy of sample films. This high sensitivity was demonstrated by J. Zhang and Grischkowsky<sup>2</sup> by detecting 20 nm thick water layers within the PPWG. Since the first demonstration of the waveguide THz-TDS technique to characterize molecular solids by Melinger *et al.*<sup>3</sup> in 2006, it has been successfully employed to extract the high resolution THz vibrational data of a variety of molecule types, ranging from organic, biological, pharmaceutical as well as explosive and energetic materials.<sup>3–10</sup> The increased resolution offered by this technique has resulted in the observation of new THz vibrational modes often hidden by various broadening mechanisms, and which for some of the explosive materials, can be compared to recent single crystal measurements at low temperatures.<sup>11,12</sup> The increased resolution has the potential to lead to better understanding and modeling of the molecular solids.<sup>13</sup>

An important issue which has not yet been studied experimentally in a systematic way is the effect of the metal surface on the THz spectrum of the polycrystalline film. Interactions between the molecular analyte and the metal surface can, in principle, alter the frequencies and intensities of the THz vibrational modes. We consider two possibilities:

The first is the potential for metal ions to incorporate into the parent organic film. In waveguide THz-TDS polycrystalline films are formed on the metal surface (often Cu, Au or Al) of the waveguide plate. When the drop casting technique is employed to cast these films, the sample solution sits on the metal plates for a finite time before crystallization occurs. This time is greatly dependent on how volatile the solvent is. The successful evaporation of the solvent leaves behind a thin polycrystalline film of high crystallinity on the metal surface. During the time the sample is in the solution phase there is a possibility of metal ions entering the solution and being incorporated within the crystalline lattice to form a molecule-metal complex. We have observed a few cases where Cu ions have become incorporated into organic films. For example, in the case where the amino acid tryptophan was drop cast from aqueous solution on Cu (during our earlier attempts to characterize bio-organic samples<sup>4</sup>), the normally colorless tryptophan solid turned blue-green, suggesting a reaction with Cu ions. The reaction was observed only when water was used as a solvent and can likely be attributed to the Cu (II)-amino acid reaction.<sup>14,15</sup> We found that the incorporation of Cu ions greatly affects the tryptophan spectrum, so that only one of the four THz resonances observed at 77 K survives. The reaction was not observed when a non-aqueous volatile solvent was used, or when Al was used as the substrate. In general, the formation of a molecule-metal complex film will depend there being sufficient metal ions present and the propensity for complexation to occur.

A second case is the potential interaction of the molecular film and the metal surface in the interfacial region. As an example, a recent theoretical study by Guadarrama-Perez *et al.*, model and analyze the interaction of the molecule RDX with an Al surface.<sup>16</sup> In that paper, the authors predict the formation of a RDX-Al complex that is mediated by the interaction between oxygen atoms of the RDX nitro groups

<sup>a)</sup>Author to whom correspondence should be addressed. Electronic mail: daniel.grischkowsky@okstate.edu.

| <b>Report Documentation Page</b>  |                                    |   | <i>Form Approved<br/>OMB No. 0704-0188</i> |                     |
|---|------------------------------------|---|--|---------------------|
| <p>Public reporting burden for the collection of information is estimated to average 1 hour per response, including the time for reviewing instructions, searching existing data sources, gathering and maintaining the data needed, and completing and reviewing the collection of information. Send comments regarding this burden estimate or any other aspect of this collection of information, including suggestions for reducing this burden, to Washington Headquarters Services, Directorate for Information Operations and Reports, 1215 Jefferson Davis Highway, Suite 1204, Arlington VA 22202-4302. Respondents should be aware that notwithstanding any other provision of law, no person shall be subject to a penalty for failing to comply with a collection of information if it does not display a currently valid OMB control number.</p> |                                    |   |  |                     |
| 1. REPORT DATE<br><b>23 JAN 2012</b>  | 2. REPORT TYPE                     | 3. DATES COVERED<br><b>00-00-2012 to 00-00-2012</b> |  |                     |
| 4. TITLE AND SUBTITLE<br><b>Substrate independence of THz vibrational modes of polycrystalline thin films of molecular solids in waveguide THz-TDS</b>  |                                    |   |  |                     |
| 5a. CONTRACT NUMBER   |                                    |   |  |                     |
| 5b. GRANT NUMBER  |                                    |   |  |                     |
| 5c. PROGRAM ELEMENT NUMBER  |                                    |   |  |                     |
| 6. AUTHOR(S)  |                                    |   |  |                     |
| 5d. PROJECT NUMBER  |                                    |   |  |                     |
| 5e. TASK NUMBER   |                                    |   |  |                     |
| 5f. WORK UNIT NUMBER  |                                    |   |  |                     |
| 7. PERFORMING ORGANIZATION NAME(S) AND ADDRESS(ES)<br><b>Oklahoma State University, School of Electrical and Computer Engineering, Stillwater, OK, 74078</b>  |                                    |   |  |                     |
| 8. PERFORMING ORGANIZATION REPORT NUMBER  |                                    |   |  |                     |
| 9. SPONSORING/MONITORING AGENCY NAME(S) AND ADDRESS(ES)   |                                    |   |  |                     |
| 10. SPONSOR/MONITOR'S ACRONYM(S)  |                                    |   |  |                     |
| 11. SPONSOR/MONITOR'S REPORT NUMBER(S)  |                                    |   |  |                     |
| 12. DISTRIBUTION/AVAILABILITY STATEMENT<br><b>Approved for public release; distribution unlimited</b>   |                                    |   |  |                     |
| 13. SUPPLEMENTARY NOTES<br><b>Sponsored in part by from Naval Research Lab grant N00173-09-2-C007.</b>  |                                    |   |  |                     |
| 14. ABSTRACT  |                                    |   |  |                     |
| 15. SUBJECT TERMS   |                                    |   |  |                     |
| 16. SECURITY CLASSIFICATION OF:   |                                    |   | 17. LIMITATION OF ABSTRACT                 | 18. NUMBER OF PAGES |
| a. REPORT<br><b>unclassified</b>  | b. ABSTRACT<br><b>unclassified</b> | c. THIS PAGE<br><b>unclassified</b>                 | <b>Same as Report (SAR)</b>                | <b>7</b>            |
| 19a. NAME OF RESPONSIBLE PERSON   |                                    |   |  |                     |

and the Al surface. From this interaction they calculate a coupling of the RDX vibrational motion to the motion of the Al atoms at the surface. The authors then predict that this interaction is one of the reasons for the additional vibrational lines resolved using the waveguide THz-TDS technique. But in a recent paper from our group, RDX was characterized using the waveguide THz-TDS technique on two different substrates namely Au-coated Cu and Al, and we have observed that the THz vibrational spectrum does not significantly change.<sup>7</sup> While this does not preclude a significant interfacial interaction, our observation shows that the bulk part of the film, which dominates the waveguide THz-TDS signal, retains the character of neat RDX.

In order to more systematically address the issues of solvent, sample and substrate interaction raised above, we present an experimental investigation to test for a substrate dependence of the observed vibrational modes with waveguide THz-TDS. The investigation of substrate dependence is performed using salicylic acid as the test molecule. This molecule has been characterized earlier and is known to have well defined and well separated vibrational modes in the THz frequency range.<sup>5,17,18</sup> The THz response of salicylic acid films is measured on three different metal substrates: Al, Cu, and Au, and on two passivated metal surfaces: Mylar on Al and a self assembled monolayer (SAM) on Au. Salicylic acid is first characterized in the pellet form and then compared to the absorption features measured using waveguide THz-TDS to verify that the absorption features measured using the PPWG match with those observed in the pellet. The molecule-metal interaction, if present, is limited to the interfacial region between and does not affect the subsequent bulk crystallization. In this limit, a signal due to molecule-metal interactions would be much smaller than the signal from the interaction of the THz field with the bulk material. The results shown here are consistent with previous waveguide THz-TDS measurements, where the THz spectra of films measured on different metal surfaces showed strong similarity in the observed line frequencies and line strengths.<sup>7-9</sup>

## II. EXPERIMENTAL SETUP

A standard THz-TDS setup based on photoconductive switches was used for sample characterization (see Fig. 1(a)). THz radiation is generated and detected using photoconductive switches driven by 10 mW optical pulse trains from an 800 nm, 80 fs, 100 MHz mode locked Ti: sapphire femtosecond laser. The emitted THz radiation is collimated by a high-resistivity Si lens and a parabolic mirror. A time domain amplitude signal to noise (S/N) ratio of 10 000 can be achieved with this system. The entire system is located in an airtight enclosure to overcome the effects of water vapor absorption on the THz beams. The system also incorporates either a LN<sub>2</sub> cryostat or a mechanical He-cryocooler coupled to a vacuum chamber to facilitate low temperature measurements.

The metal PPWGs used for waveguide THz-TDS in this study were fabricated using standard machining tolerances (see Fig. 1(b)). The dimensions of the two metal plates are 28 mm (width)  $\times$  30 mm (length)  $\times$  10 mm (thickness). The

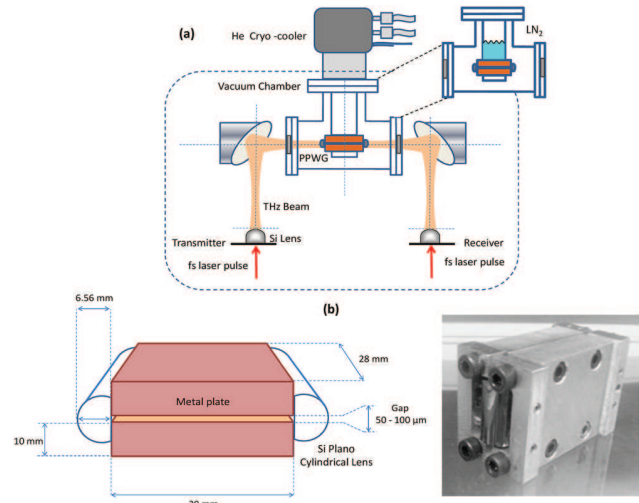


FIG. 1. (Color online) (a) Waveguide THz-TDS system with cryogenic capability (both He-Cryocooler and LN<sub>2</sub> cooling setups shown). (b) Metal parallel plate waveguide used for waveguide THz-TDS.

inner surfaces were polished to a mirror finish. The PPWG assembly with a 50  $\mu$ m gap was obtained by placing four metal spacers at the corners of each of the plates. THz pulses are coupled into and out of the PPWG using plano-cylindrical high resistivity Si lenses at the entrance and exit faces of the PPWG assembly. The lenses are 15 mm (height)  $\times$  10 mm (width)  $\times$  6.56 mm (thickness), with a 5 mm radius of curvature. The PPWG was operated in the TEM mode which exhibits nondispersive and low loss THz pulse propagation.<sup>1</sup> The polarization of the THz field is perpendicular to the waveguide surface. Typical amplitude transmission efficiency through the 50  $\mu$ m gap PPWG is within the range of 20%–25% for frequencies near 1 THz without the cryo-cooler assembly.

In order to study the substrate dependence of the vibrational modes, three different metal surfaces were chosen namely Al, Cu, and Au. In addition, these three metallic substrates were compared to two neutral substrates, a dielectric 2.5  $\mu$ m thick Mylar covered Al plate and a self-assembled monolayer (SAM) formed on an Au coated Si chip, which is incorporated within a Cu PPWG. The Mylar covered Al substrate was made by carefully stretching a commercially available 2.5  $\mu$ m thick Mylar sheet over the surface of an Al waveguide plate and securing it using adhesive tape on the back. These two passivated substrates represent two different passivation techniques namely a simple mechanical passivation using a dielectric (Mylar) and the other a molecule specific passivation through SAMs. The ultrathin ( $\sim$ 1–2 nm) SAM layer can lead to surface passivation without the extra broadband absorption introduced by the relatively thick Mylar layer. The SAM used here is 11-hydroxy-undecanethiol (Asemlon, 97%) on an Au-coated Si chip (15 mm  $\times$  30 mm).

The amplitude transmission spectra through the PPWGs made of four different materials, Al, Cu, Au coated Cu and Mylar coated Al, and with no sample in place, is compared in Fig. 2. All the metal PPWGs exhibit good TEM mode propagation, with a spectral throughput extending all the

way up to 4 THz. The Au coated Cu PPWG has the maximum spectral amplitude transmission. The Mylar covered PPWG supports single TEM mode propagation and only introduces a minor dispersion and broadband absorption above 1 THz, due to the 2.5  $\mu\text{m}$  thick layer. The high frequency components are attenuated by the Mylar layer, and we obtain measurable amplitude transmission only up to 2.5 THz. But the clean TEM mode propagation through this PPWG provides for an easy way to make a neutral substrate for waveguide THz-TDS.

The salicylic acid pellets were made by making a uniform mixture of 27 mg of salicylic acid and 330 mg of polyethylene powder and then compressing this mixture into a 2 mm thick by 10 mm diameter pellet using a hydraulic press applying a pressure of 11 metric tons. The polycrystalline films on the waveguide plates were made by the drop-casting technique from a 10 mg/ml salicylic acid solution in acetone. Prior to the drop casting, the non-passivated metal substrates were cleaned in oxygen plasma for 2 min. Approximately 250  $\mu\text{l}$  of the solution was deposited on the substrates and then the solvent was allowed to evaporate to obtain a thin polycrystalline film. The thick edges were swabbed to leave a 1.5 cm  $\times$  1.5 cm (approx.) sample layer. These waveguide plates were then incorporated into a PPWG using matching plates and 50  $\mu\text{m}$  spacers. In the case of the sample on the SAM-coated surface, the 15 mm  $\times$  30 mm Si chip is inserted between the two matching plates and forms one of the inner surfaces of the PPWG. The Si lenses are then attached to the system as shown in Fig. 1. The PPWG assembly is then introduced into the cryostat and the temperature dependent characterization is performed in the THz system. All the waveguides were cooled to 13 K and their THz amplitude absorption spectrum was measured. The sample temperature was measured by a Si diode temperature sensor attached to the waveguide. To extract the amplitude absorbance, a reference,  $A_{\text{ref}}$ , was estimated by fitting the amplitude spectra  $A_{\text{spec}}$ , at points away from any sharp features with a spline. The amplitude absorbance was then calculated via the expression:  $\text{Absorbance} = -\ln[A_{\text{spec}}/A_{\text{ref}}]$ .

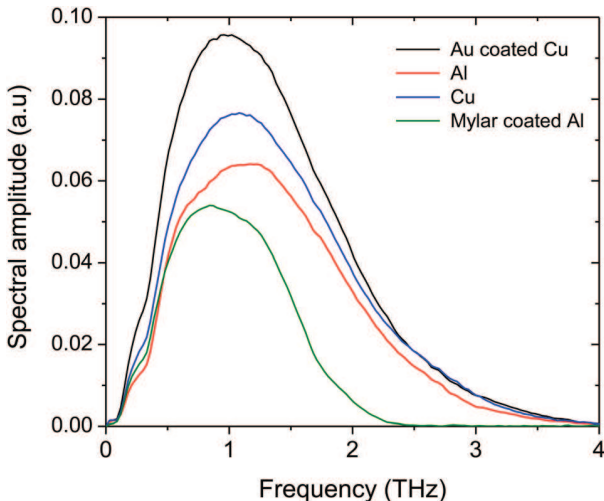


FIG. 2. (Color online) Comparison of spectral amplitude transmission through the PPWG with different substrates.

X-ray diffraction (XRD) analysis of the thin films on metal and mylar surfaces was performed using a Rigaku 18 kW x-ray generator and a high resolution powder diffractometer. To approximate a powder spectrum we thoroughly mixed finely ground salicylic acid powder in apiezon grease and then spread a thin film of the mixture on a microscope slide. For all samples, the diffracted beam was analyzed by a graphite crystal to remove the Cu-K-beta component and the diffracted intensity was recorded as a function of  $2\theta$ .

### III. RESULTS AND DISCUSSION

The amplitude transmission spectrum of the salicylic acid film within a Cu PPWG is shown in Fig. 3. The room temperature measurement shows the evidence of absorption features around 1 and 2 THz. Upon cooling the PPWG to lower temperatures we can see the evolution of the absorption features. At 80 K the transmission spectrum reveals the presence of 7 vibrational modes which considerably narrow compared to the linewidths observed at room temperature. Cooling down to 13 K results in further line narrowing and results in a well resolved vibrational fingerprint associated with the salicylic acid molecule. The absorbance of the salicylic acid film at 80 K is compared in Fig. 4 to that of the salicylic acid - PE pellet, obtained by cooling the pellet to 80 K. It is clear from the figure that the modes observed from the pellet measurement are reproduced in the waveguide data, except for the one at 2.9 THz. The relative intensities are different in the film which is likely due to polarization effects resulting from the preferential orientation of the microcrystals with respect to the propagating THz field within the PPWG.

Figure 5 shows the XRD spectrum obtained in the Bragg-Brentano ( $\theta$ - $2\theta$ ) configuration for polycrystalline salicylic acid films on each of the substrates. For the film on the Mylar-passivated surface we have increased both the slit width and acquisition time by a factor of 2 to boost the signal. For comparison, we also show the experimental powder spectrum for salicylic acid measured on the same instrument, as well as the calculated powder spectrum taken from the

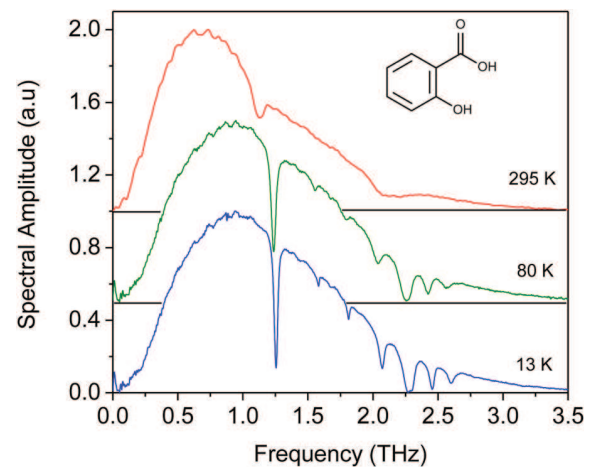


FIG. 3. (Color online) Transmitted THz amplitude spectrum of the salicylic acid film within the Cu PPWG measured at 295 K, 80 K and 13 K. The curves for the 80 K and 295 K measurement have been vertically shifted for clarity.

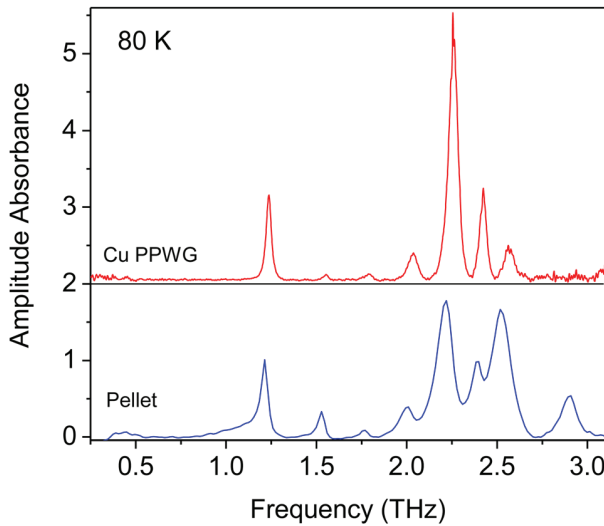


FIG. 4. (Color online) Comparison of the absorbance of the salicylic acid-PE pellet to that of salicylic acid polycrystalline film within a Cu PPWG at 80 K. The Cu PPWG measurement has been vertically shifted for clarity.

Cambridge Crystallographic Data Center (Mercury 2.4). Salicylic acid crystallizes in the monoclinic system having a space group  $P2_1/a$  with 4 molecules per unit cell.<sup>19</sup> The optical micrographs of these films on all the substrates are shown in Fig. 6. For the XRD measurement, the source used Cu-k-alpha radiation (1.5405 Å) and an x-ray illumination area of 1 cm<sup>2</sup>. From the x-ray data it is clear that the film exhibits similar preferential orientation on all the substrates. Comparing the optical micrographs of microcrystals of salicylic acid on each of the substrates, we can see a strong similarity in the microcrystal shape and sizes. Clusters of thin, long, needle like crystals of length  $\sim 200$ – $300$   $\mu\text{m}$  are obtained. Upon comparison to the powder spectra we conclude that the films on all the substrates show a preferential orientation along the (110) direction with a corresponding strong peak at 10.96° and the next stronger peak at 17.22° corresponding to the (210) planes. We also see very weak peaks at 15.26°, 15.74°, 17.56°, 28.02° and 33.34° which closely match to the data base values observed for pure salicylic acid. We note that the most intense peak in the predicted powder XRD spectrum is due to the (121) plane and occurs near  $2\theta = 25.4$ °. This peak is not observed in the XRD of the film, presumably due to the preferred orientation of the film on the surface.

A more quantitative estimate of the preferred orientation may be obtained from the March-Dollase method.<sup>20,21</sup> Here, the so-called March parameter,  $r$ , is related to the fraction of crystallites which exhibit a preferred orientation along a crystalline plane, and is calculated from the equation:<sup>21</sup>

$$r = \left[ \frac{\sin^2 \alpha}{\left( (\kappa/\kappa_p)^{2/3} - \cos^2 \alpha \right)} \right]^{1/3}, \quad (1)$$

where  $\alpha$  is the angle between the plane of preferred orientation and a comparison plane,  $\kappa$  is the observed intensity ratio of the diffraction peaks of these planes (in the film), and  $\kappa_p$  is the corresponding intensity ratio of the two planes from the random powder spectrum. A complete preferred orientation will give

$r = 0$ , while a fully random orientation will give  $r = 1$ . It has been shown that the degree of preferred orientation, called  $\eta$ , may be obtained from  $r$  using the equation,<sup>21</sup>

$$\eta = 100\% \left[ \frac{(1-r)^3}{(1-r^3)} \right]^{1/2}. \quad (2)$$

To calculate  $\eta$  for the (110) plane we use the (210) plane as a comparison plane. The angle  $\alpha$  between (110) and (210) is calculated from the standard formula for a monoclinic cell<sup>22</sup> and found to be 18.50°. The intensity ratio  $\kappa_p$  is found from the calculated powder spectrum (Fig. 5). For the films on Au, Al, and Cu,  $r = 0.24, 0.31, 0.43$ , respectively, and  $\eta = 67\%, 58\%$ , and 44%, respectively. The most highly textured film is on Au, with decreasing texture for the films on Al and then Cu. For performing the XRD measurements a Si wafer coated with Au was used as a substrate. The Si surface is much smoother than the bulk Al and Cu plates, which allows a higher degree of orientation of microcrystals with respect to the surface normal.

The salicylic acid film cast on the SAM-coated Au surface shows similar preferential orientation on the (110) plane. There is an additional peak near  $2\theta = 33$ ° which is due to a slight exposure of the Si substrate to the x-ray beam. We mention that there is some evidence that SAMs with appropriate end groups can induce a unique preferred orientation of microcrystals on a surface.<sup>23</sup> However, the x-ray spectrum shows that the 11-hydroxy-undecanethiol SAM does not produce a significantly different orientation for the salicylic acid film on the surface.

With these results in mind, the absorbance spectrum at 13 K obtained from the waveguide THz-TDS measurements of salicylic acid films on each of the substrates is compared in Fig. 7. In each case, we see that upon cooling the resonances have undergone significant line narrowing in comparison to room temperature measurements. The films on all the substrates, namely the three metal and the two passivated substrates, exhibit very similar absorbance spectra. The line-centers of the vibrational modes measured for the films on each of the substrates using waveguide THz-TDS are collected in Table I. The line centers are determined with a precision of 1 GHz. The highest precision is achieved around the spectral region of 1 THz (where the source has the maximum spectral amplitude (and high S/N ratio) and falls off on either side of the spectrum as the S/N drops as one moves away from this spectral region). A minor exception is the film on the SAM-coated surface, which reveals two additional resonances near 2.77 and 2.90 THz. These lines have appeared in earlier waveguide THz-TDS measurements,<sup>5</sup> and also in the pellet measurements of references.<sup>17,18</sup> As evident from Table I and Figs. 5 and 7, we have achieved a remarkable reproducibility of the vibrational mode frequencies for salicylic acid on all substrates including Mylar and the SAM passivated waveguide. There is somewhat less uniformity in the relative line intensities shown by the different films. This may be due to differences in the net orientation of microcrystals on each surface. It is not clear why two additional modes were observed in the case of the film on the SAM-coated surface. This may be

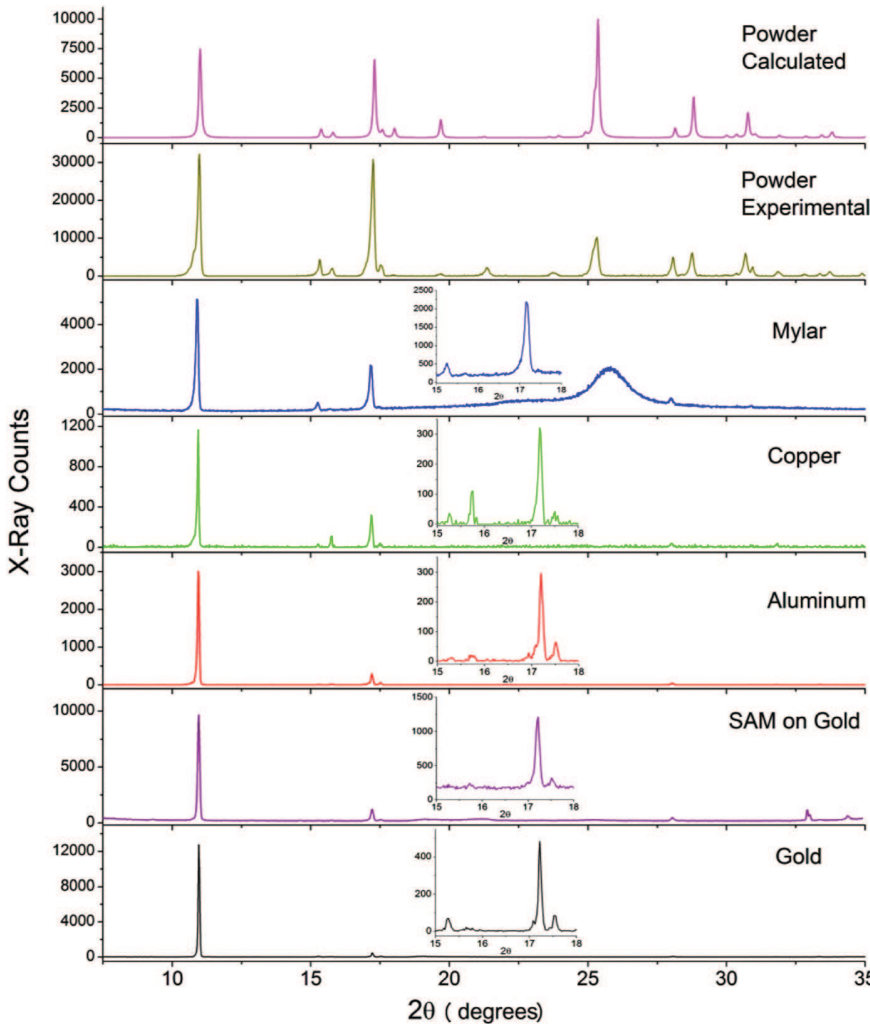


FIG. 5. (Color online) Comparison of the XRD data obtained for the salicylic acid polycrystalline film on various substrates, and experimental and calculated powder spectra. The SAM on gold is 11-hydroxy-undecanethiol. The table compares the XRD line centers observed to that from a database and the respective crystal planes are also listed.

| 2θ (Database) | 2θ (Observed) | Crystal plane |
|---------------|---------------|---------------|
| 11.05         | 10.96         | (110)         |
| 15.37         | 15.26         | (210)         |
| 15.81         | 15.74         | (020)         |
| 17.30         | 17.22         | (210)         |
| 17.60         | 17.56         | (120)         |
| 28.19         | 28.08         | (320)         |
| 33.47         | 33.34         | (330)         |

simply that the film is more highly textured on the much smoother surface provided by the Au-coated Si chip compared to the standard “hand-polished” surfaces of the metal waveguides. These results show that for salicylic acid, if a significant molecule-metal interaction occurs then its contribution compared to the bulk signal is relatively small and is not resolved with the current sensitivity of the experiment. Therefore, the vibrational modes observed are indeed that of the analyte.

To determine the extent that the current configuration of waveguide THz-TDS can detect a molecule-metal interaction confined to the interfacial region, we estimate the size of the

interfacial region of the film affected by the interaction with respect to the bulk part of the film. If the polycrystalline salicylic acid film (density of  $1.443 \text{ g/cm}^3$ ) with mass of 200 micrograms is spread uniformly over the  $1.5 \text{ cm} \times 1.5 \text{ cm}$  footprint, its equivalent layer thickness would be approximately 600 nm. For a molecule-metal interaction that is confined to the interface, such as the collective vibrational motion of the molecule with metal surface atoms (as studied in Ref. 16), it seems reasonable to assume that the depth of the molecular crystal affected would be at most a few unit cells deep. The largest unit cell dimensions are  $11.52 \text{ \AA}$  along the  $a$ -axis and  $11.21 \text{ \AA}$  along the  $b$ -axis,<sup>18</sup> so that the interfacial region of the molecular crystal affected by

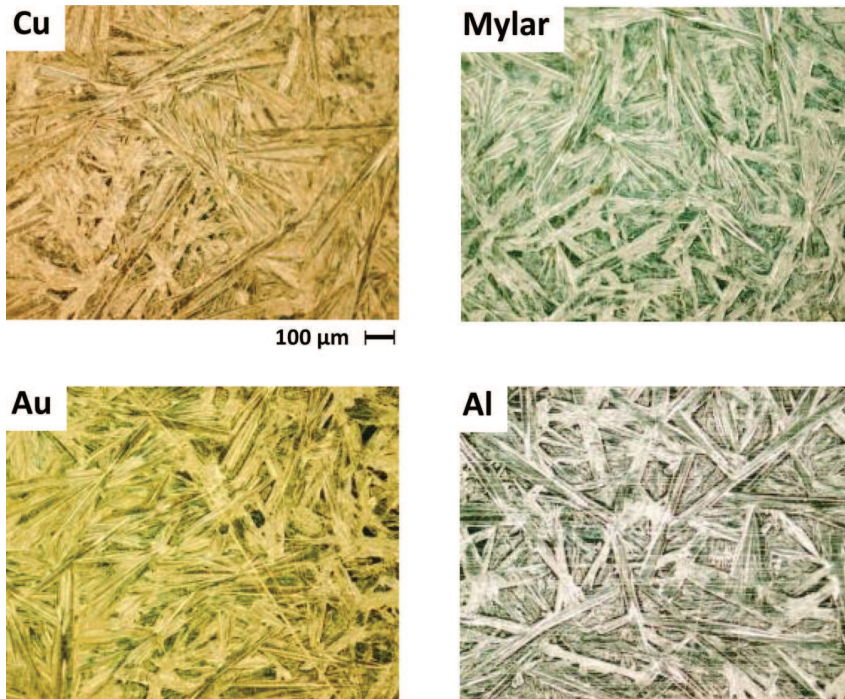


FIG. 6. (Color online) Optical micrographs of salicylic acid dropcast films on four different substrates namely Cu, Mylar, Au and Al. Scale bar applies to all the micrographs.

interactions with the metal surface might be a few nanometers deep. This depth is small compared to the estimated 600 nm thickness of a uniform bulk layer. At the current sensitivity, waveguide THz-TDS can resolve absorption signals as small as about 1–2%. With this sensitivity, THz modes due to molecule-metal interactions could only be observed if these modes have strong line intensities with respect to the bulk THz modes.

The results obtained here for salicylic acid are consistent with our previous observations of substrate independence of organic films on different metal surfaces. These comparisons have been presented in earlier publications for the explosives

molecules RDX, HMX, and TNT, and the organic solids 4-iodo-nitrobiphenyl (4INBP) and tetracyanoquinodimethane (TCNQ),<sup>7–9</sup> where the characterizations were done on at least two different metals to compare the THz vibrational spectra and to rule out the effect of molecule-metal interaction. For these previous cases and the results here for salicylic acid, the observed independence of the THz spectrum to the substrate shows that any effects due to the molecule-metal interaction were confined to the interfacial region and did not propagate into the bulk portion of the film which is probed by waveguide THz-TDS.

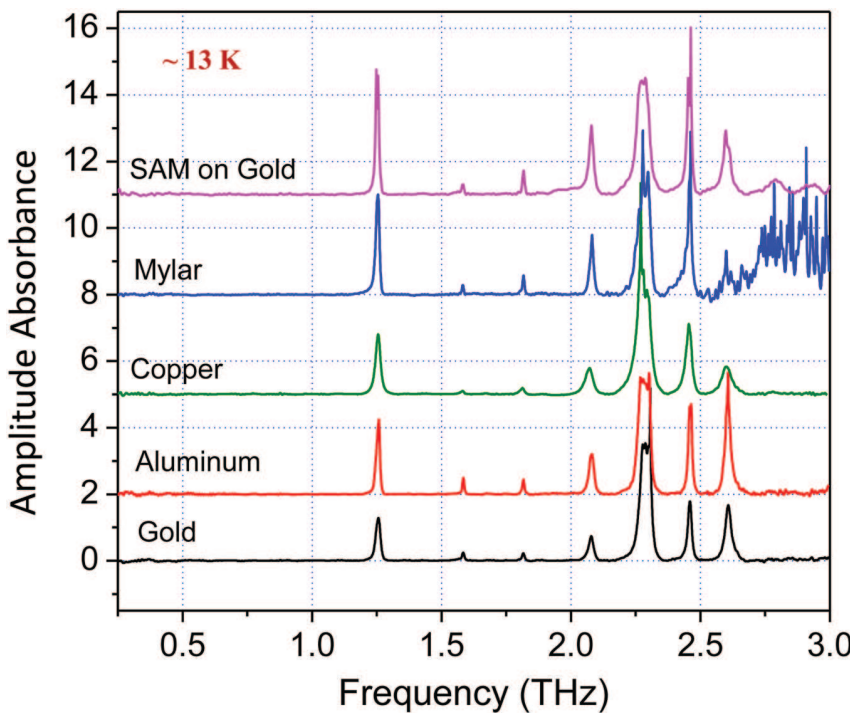


FIG. 7. (Color online) Comparison of the THz vibrational modes for salicylic acid obtained using waveguide THz-TDS for different substrates within the PPWG. The absorbance plots are vertically shifted for better clarity.

TABLE I. Comparison of the line-centers (THz) at 13 K of the vibrational modes measured on different substrates using waveguide THz-TDS.

| Gold  | Aluminum | Copper | Mylar | SAM   |
|-------|----------|--------|-------|-------|
| 1.256 | 1.258    | 1.256  | 1.255 | 1.252 |
| 1.584 | 1.584    | 1.582  | 1.583 | 1.583 |
| 1.816 | 1.817    | 1.813  | 1.817 | 1.817 |
| 2.079 | 2.081    | 2.072  | 2.081 | 2.079 |
| 2.29  | 2.29     | 2.28   | 2.29  | 2.28  |
| 2.459 | 2.461    | 2.455  | 2.460 | 2.459 |
| 2.608 | 2.607    | 2.600  | 2.60  | 2.604 |
| –     | –        | –      | –     | 2.790 |
| –     | –        | –      | –     | 2.920 |

Our main conclusion is that for a given crystalline analyte it is relatively straight forward to choose the appropriate conditions for casting a polycrystalline film on a metal surface so that the THz spectrum obtained by waveguide THz-TDS is that of the bulk analyte, and not that of a material altered by a molecule-metal interaction. In cases where volatile solvents such as acetone, methanol, and chloroform can be used for drop casting, the solution remains on the metal surface for a relatively short time and thereby minimizes interactions with metal ions in solution. The use of non-polar solvents such as toluene also minimizes the introduction of metal ions in solution. In addition, we have demonstrated that dielectric covered metal PPWG's and SAM-passivated metal PPWG's maintain good TEM mode propagation. Such passivated metal surfaces can be used as a neutral substrate for forming polycrystalline films for materials to have known reactivity to metals, and the full potential of waveguide THz-TDS in characterizing molecular solids can be realized.

#### IV. SUMMARY

Using waveguide THz-TDS with three metal substrates and two passivated metal substrates namely dielectric coated and SAM coated, we have shown that the observed THz vibrational modes of a molecular film are independent of the substrate used. This independence of the vibrational modes on the substrate shows that either there is no interaction of the substrate with the analyte, or that the interaction, even if present, is confined to the molecular layers closest to the metal and at the current S/N is not thick enough to be sensed by the THz radiation propagating through the waveguide. The microcrystals formed in the polycrystalline film in the PPWG are of high crystalline quality and are responsible for the well resolved vibrational resonances observed at

cryogenic temperatures. In addition, passivated metal PPWG's can be used to characterize analyte molecules with known reactivity to metals.

#### ACKNOWLEDGMENTS

The authors thank Alisha J. Shutler of Oklahoma State University for assistance with waveguide measurements. This work was partially supported by the National Science Foundation, the Defense Threat Reduction Agency (11-2210M), and the Office of Naval Research.

- <sup>1</sup>R. Mendis and D. Grischkowsky, *Opt. Lett.* **26**, 846 (2001).
- <sup>2</sup>J. Zhang and D. Grischkowsky, *Opt. Lett.* **19**, 1617 (2004).
- <sup>3</sup>J. S. Melinger, N. Laman, S. Sree Harsha, and D. Grischkowsky, *Appl. Phys. Lett.* **89**, 251110 (2006).
- <sup>4</sup>N. Laman, S. Sree Harsha, D. Grischkowsky, and J. S. Melinger, *Biophys. J.* **94**, 1010 (2008).
- <sup>5</sup>N. Laman, S. Sree Harsha, and D. Grischkowsky, *Appl. Spect.* **62**, 319 (2008).
- <sup>6</sup>J. S. Melinger, N. Laman, and D. Grischkowsky, *Appl. Phys. Lett.* **93**, 011102 (2008).
- <sup>7</sup>J. S. Melinger, S. Sree Harsha, N. Laman, and D. Grischkowsky, *J. Opt. Soc. Am. B*, **26**, A79 (2009).
- <sup>8</sup>J. S. Melinger, S. Sree Harsha, N. Laman, and D. Grischkowsky, *Opt. Exp.* **18**, 27238 (2010).
- <sup>9</sup>N. Laman, S. Sree Harsha, D. Grischkowsky, and J. S. Melinger, *Opt. Exp.* **16**, 4049 (2008).
- <sup>10</sup>J. S. Melinger, N. Laman, S. Sree Harsha, S. Cheng, and D. Grischkowsky, *J. Phys. Chem. A* **111**, 10977 (2007).
- <sup>11</sup>V. H. Whitley, D. E. Hooks, K. J. Ramos, J. F. O'Hara, A. K. Azad, A. J. Taylor, J. Barver, and R. D. Averitt, *Anal. Bioanal. Chem.* **395**, 315 (2009).
- <sup>12</sup>V. H. Whitley, D. E. Hooks, K. J. Ramos, T. H. Pierce, J. F. O'Hara, A. K. Azad, A. J. Taylor, J. Barber, and R. D. Averitt, *J. Phys. Chem. A* **115**, 439 (2011).
- <sup>13</sup>K. C. Oppenheim, T. M. Korter, J. S. Melinger, and D. Grischkowsky, *J. Phys. Chem. A* **114**, 12513 (2010).
- <sup>14</sup>P. A. Korber and K. Sugiura, *J. Biol. Chem.* **8**, 1 (1912).
- <sup>15</sup>R. M. Izatt, J. S. Christensen, and V. Kothari, *Inorg. Chem.* **3**, 1565 (1964).
- <sup>16</sup>C. Guadarrama-Prez, J. M. Martnez de La Hoz, and P. B. Balbuena, *J. Phys. Chem. A* **114** (6), 2284 (2010).
- <sup>17</sup>M. Walther, "Modern Spectroscopy on Biological Molecules: Structure and Bonding Investigated by THz Time-Domain and Transient Phase-Grating Spectroscopy," Ph.D.dissertation (Albert Ludwigs Universität, Freiburg, Freiburg Germany, 2003).
- <sup>18</sup>M. Walther, P. Plochocka, B. Fischer, and P. U. Jepsen, *Biopolymers* **67**, 310 (2002).
- <sup>19</sup>W. Cochran, *Acta Cryst.* **6**, 260 (1953).
- <sup>20</sup>W. A. Dollase, *J. Appl. Cryst.* **19**, 267 (1986).
- <sup>21</sup>E. Zolotoyabko, *J. Appl. Cryst.* **42**, 513 (2009).
- <sup>22</sup>B. D. Cullity, *Elements of X-ray Diffraction* (Addison-Wesley Reading, MA, 1978), p. 503.
- <sup>23</sup>A. L. Briseno, J. Aizenburg, Y. J. Han, R.A. Penkala, H. Moon, A. J. Moon, A. J. Lovering, C. Kloc, and Z. Bao, *J. Am. Chem. Soc.* **127**, 12164 (2005).